IEEE Photonics Journal
An IEEE Photonics Society Publication

Open Access

An optical Fiber Pressure Sensor With Ultra-Thin Epoxy Film and High Sensitivity Characteristics Based on Blowing Bubble Method

Volume 13, Number 1, February 2021

Shubin Zhang
Qi Lei
Jiabin Hu
Yubo Zhao
Haitao Gao
Jian Shen
Chaoyang Li

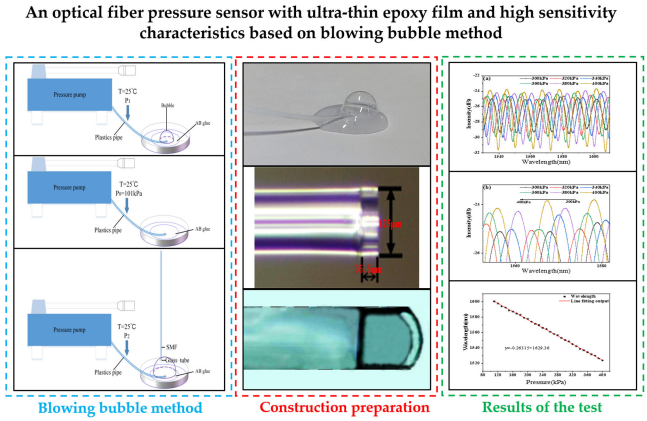

DOI: 10.1109/JPHOT.2021.3055872

An optical Fiber Pressure Sensor With Ultra-Thin Epoxy Film and High Sensitivity Characteristics Based on Blowing Bubble Method

Shubin Zhang,[1,2] **Qi Lei**,[2] **Jiabin Hu**,[1,2] **Yubo Zhao**,[1,2] **Haitao Gao**,[1,2] **Jian Shen**,[1,2] **and Chaoyang Li**[1,2]

[1]State Key Laboratory of Marine Resource Utilization in South China Sea, Hainan University, Haikou 570228, China
[2]School of Information and Communication Engineering, Hainan University, Haikou 570228, China

DOI:10.1109/JPHOT.2021.3055872
This work is licensed under a Creative Commons Attribution 4.0 License. For more information, see https://creativecommons.org/licenses/by/4.0/

Manuscript received November 20, 2020; revised January 20, 2021; accepted January 27, 2021. Date of publication February 8, 2021; date of current version February 15, 2021. This work is supported by Hainan Provincial Natural Science Foundation of China (2019RC054) and Dongguan Introduction Program of Leading Innovative and Entrepreneurial Talents. Corresponding authors: Jian Shen; Chaoyang Li (e-mail: shenjian@hainanu.edu.cn; lichaoyang@hainanu.edu.cn).

Abstract: In this paper, an implementation method of high sensitivity thin film fiber optic pressure sensor based on air blowing method is proposed. The utility model is characterized in that a film ultra-thin microbubble structure is firstly formed on the surface of the AB epoxy glue solution by using high-pressure air, and then the film portion of the end portion of the microbubble is transferred to a single-mode fiber head with a hollow glass tube at the top. Finally, a thin film structure fiber Fabry-Perot fiber pressure sensor is formed. The experimental results show that the thickness of the thin film layer at the end of the FP sensor is only 16 μm. Correspondingly, the maximum pressure sensitivity can reach 263.15 pm/kPa. Meanwhile, due to the decrease of film thickness, the sensor's resistance to temperature interference is improved. The prepared fiber Fabry-Perot pressure sensor has the advantages of ultra-thin film thickness, high-pressure sensitivity, low cost and good repeatability. Therefore, it has good application value in high sensitivity pressure and sound wave detection.

Index Terms: Bubble blowing method, Fiber optic pressure sensor, AB epoxy glue.

1. Introduction

Optical fiber F-P cavity pressure sensor is widely used in physical and biochemical parameters measurement due to its advantages such as high sensitivity, small size, anti-electromagnetic field interference, etc [1]. For example, in the medical field, the use of fiber optic pressure sensors for measurement of intracranial pressure, chest pressure, abdominal pressure can minimize the risk of surgery [2]–[4]. In biomedical science, the optical fiber medical sensors with integrated high-tech technology have attracted much attention in the life sciences, for example, to solve the oropharyngeal dysphagia caused by pathological aging and physiological aging [5]–[7]. The measurement accuracy and sensitivity of the FP pressure sensor have been improved to some extent, and linearity can be as high as $\pm$0.5% [8]. Since the 1990s, optical fiber FP pressure

sensors have entered the practical stage [9]. In 2005, Ken K. Chin of the New Jersey Institute of Technology in the United States combined with MEMS technology to fabricate a diaphragm-type fiber optic sensor using an ultra-sensitive diaphragm measuring 3 mm∗3 mm∗530 μm. The static pressure sensitivity of the sensor is 1.187 nm/Pa [10]. In 2010, L.H. Chen *et al.* of Nanyang Technological University used a chitosan material to produce a diaphragm-type fiber-optic acoustic wave sensor with a diaphragm thickness of only 1.5 μm. The sensitivity of the sensor at 1 kHz was 0.0002 V/mPa [10]. In 2012, Fawen Guo and others at the University of Lincoln in the United States used silver diaphragms to process EFPI sensors using a silver diaphragm with a thickness of 300 nm and a diameter of 75 μm. The static pressure sensitivity of the sensor was 1.6 nm/kPa and the resonance frequency was 1.44 MHz [11]. In 2014, the EFPI sound pressure sensor processed by the Shi Xiaolong team of Anhui University using a silver diaphragm with a thickness of 150 nm and a diameter of 2.5 mm. Its sensitivity reaches 160 nm/Pa, and the minimum detectable sound pressure is 14.5 μPa/Hz$^{1/2}$ [12]. In 2015, Bing Sun *et al.* proposed a FPI-based sensing device by forming an aggregate cap on the end face of an optical fiber to form an F-P cavity. Experimental results show that the structure has a high temperature sensitivity of 249 pm/°C and a pressure sensitivity of 1130 pm/MPa, and has different sensitivity at long wave and short wave [13]. In 2016, Feifan Yu *et al.* of Tsinghua University used a MoS2 with a diameter of 125 μm and a thickness of 2 nm as a sound pressure sensitive diaphragm to obtain a sound pressure sensor with a sensitivity of 89.3 nm/Pa [14]. In general, the fiber optic pressure sensors currently studied are mainly divided into sidewall pressure sensing and diaphragm pressure sensing. The sensitivity of the sidewall type F-P pressure sensor is mainly determined by the wall thickness of the F-P cavity. However, since the cavity cannot be changed greatly, it is generally only used as a low-sensitivity large-range pressure sensor. The sensitivity of the diaphragm type F-P pressure sensor is determined by the thickness of the film thickness, but the diaphragm manufacturing process is immature and costly [15]–[17]. The sensitivity is greatly increased but the structure still needs improvement.

In addition, AB epoxy glue is a good film preparation material, which has certain toughness, good acid and alkali resistance, moisture proof, waterproof, oil and dust resistance, heat and humidity resistance and atmospheric aging. Our research showed that an ultra-thin microbubble was generated on the surface of AB epoxy adhesive by high-pressure gas, and then a fiber Fabry-Perot sensor could be fabricated based on the microbubble by the transfer method. An AB epoxy film-type fiber optic pressure sensor based on bubble blowing method is proposed. The sensor cavity is made by welding a small length of glass tube at the end of the SMF [18]–[19]. By using a pressure pump to pressurize and blow bubbles, a very thin film microbubble structure is formed on the surface of liquid AB epoxy glue, and then the film microbubbles are clicked on the end face of the glass tube to form a fiber optic F-P pressure sensor with a thin film structure. Since the AB film layer is very thin, this sensor can achieve high-pressure sensitivity with a maximum pressure sensitivity of about 263.15 pm/kPa.

2. Sensor Structure and Principle

The basic structure of the fiber optic F-P pressure sensor is a low-fineness Fabry-Perot interferometer. A well-polished lead-in fiber end face forms an F-P cavity with the inner surface of the pressure sensitive film. The internal surface of the diaphragm and the end face of the single-mode fiber constitute two cavity surfaces of the Fabry-Perot cavity. The light from the laser source is coupled to the core of the single-mode optical fiber and partially reflected when it reaches the two cavity surfaces of the diaphragm sensor. Eventually, a double-beam FP interference will be formed. Schematic diagram of the sensor head structure is shown in Fig. 1.

According to the principle of elastic deformation of the film, the pressure-sensitive film is deformed under the action of external pressure, thereby changing the length of the FP cavity and causing the change of the interference spectrum. By measuring the interference spectrum and demodulating the interference spectrum, the pressure sensitive film can be obtained. According to the principle of elastic mechanics, the relationship between pressure change and cavity length

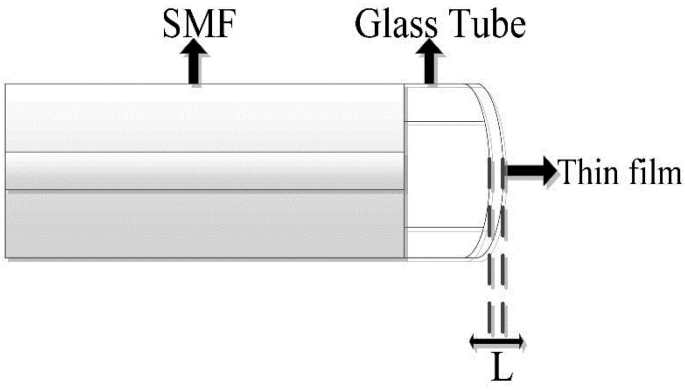

Fig. 1. Schematic diagram of the sensor head.

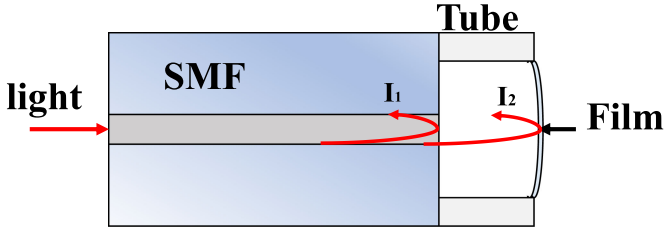

Fig. 2. The fiber Fabry-Perot pressure sensor.

change can be expressed by the following formula:

$$\Delta \mathrm{d} = \frac{3}{16}\frac{(1-\mu^2)\mathrm{r}^4}{E\mathrm{h}^3}\Delta \mathrm{p} \tag{1}$$

Where Δp is the amount of change in the pressure difference between the inside and outside of the diaphragm; h is the thickness of the film; r is the effective radius of the film; Δd is the amount of change in cavity length; μ is the Poisson's ratio of the film, and E is Young's modulus of the film. The measurement sensitivity Y is

$$Y = \frac{\Delta \mathrm{d}}{\Delta \mathrm{p}} = \frac{3}{16}\frac{(1-\mu^2)\mathrm{r}^4}{E\mathrm{h}^3} \tag{2}$$

It can be seen that the pressure measurement sensitivity is proportional to the fourth power of the effective radius of the sensitive film, and inversely proportional to the third power of the diaphragm thickness. After the material is selected, the pressure measurement sensitivity is determined by the thickness and radius of the diaphragm.

As the membrane is derived from the microbubble cavity, its structural characteristics also determine that the thickness of the central position of the membrane is relatively thinner, which enables the measurement of higher sensitivity. The two-beam interference equation is expressed as:

$$I_{\mathrm{r}} = I_1 + I_2 + 2\sqrt{I_1 I_2}\cos\left(\Delta\varphi + \varphi_0\right) \tag{3}$$

Where I_1 and I_2 are the intensities reflected by the glass-air interface and air-glass interface, φ_0 represents the initial phase, φ_0 is the optical phase difference between the two reflected light beams, which can be described as:

$$\Delta\varphi = 4\pi nL \div \lambda \tag{4}$$

In this equation, n is the refractive index of air, L is the length of the air-cavity, λ is the optical wavelength in vacuum.

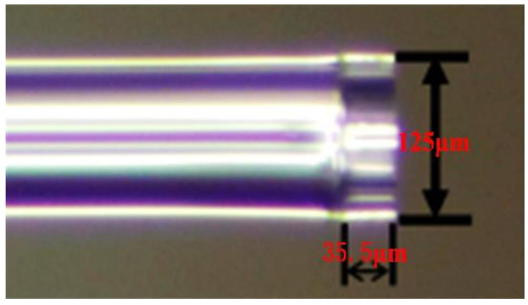

Fig. 3. Physical diagram of the structure of the fiber glass tube.

At positions of dips in the interference spectrum, the phase difference between the two reflected light beams meets the following condition:

$$\varphi = \varphi_0 + \Delta\varphi = \varphi_0 + 4\pi nL \div \lambda_m \tag{5}$$

$$\varphi = (2m+1)\,\pi, m = 1, 2, 3\ldots \tag{6}$$

The FSR (free spectral range) of the interference spectrum is:

$$FSR = \lambda_m - \lambda_{m-1} \tag{7}$$

Where, m is the integer and λ_m is the wavelength of the mth order interference dip. When axial contact force is applied to the FPI, the air-cavity length will decrease, generating wavelength shift of the interference dip. The wavelength shift amount of the m th order interference dip can be expressed as:

$$\Delta\lambda_m = \lambda_m \Delta L \div L \tag{8}$$

3. Preparation Method and Effect of Sensor

The fiber optic pressure sensor proposed is an F-P type fiber sensor. The manufacturing process of the sensor head is as follows: firstly, a quartz glass tube is welded on the end face of the cut single-mode fiber by a fusion splicer, and the cutter is controlled under an industrial microscope to cut the glass tube into a suitable cavity length. The cavity length of the glass tube used ranges from 30 μm to 60 μm. And an ultra-thin microbubble is generated on the surface of liquid AB epoxy adhesive by blowing method. As a pressure sensitive film, the film is elastic and can be used as a pressure sensor. When the microbubbles are not solidified, part of the film layer can be covered by a transfer method on a single-mode fiber head with a hollow glass tube at the end. The single-mode fiber, the glass tube, and the air layer constitute the FP cavity portion of the fiber pressure sensor, and the length of the glass tube is the cavity length of the FP cavity. This formed a new type of fiber optic Fabry-Perot fiber optic pressure sensor. The hollow fiber glass tube structure is filled with AB epoxy glue, which is characterized in that a glass tube with a length of 30 μm-60 μm micrometers is welded at the end of the fiber, and the structure of the fiber glass tube is as shown in Fig. 3. Then an ultra-thin microbubble is generated on the surface of the AB epoxy glue by using a high-pressure gas, and then the ultra-thin microbubble partial film layer is covered by a transfer method to a single-mode optical fiber head having a hollow glass tube at the end. A portion of the AB epoxy film layer having a film thickness L is formed at the end of the fiber glass tube. The blowing and membrane transfer processes are shown in Fig. 4(a)∼Fig. 4(c) respectively. The physical diagram of the samples after the transfer experiment is shown in Fig. 5. Three elements can be observed from Fig. 4: single mode fiber, glass tube, and AB epoxy film. The AB epoxy film is attached to the end of the glass tube by a bubble blowing technique. Thus, the single mode fiber core/glass tube and the glass tube/film interface form an FP cavity, and the reflected light creates an interference pattern on the FP cavity. The single mode fiber directs the

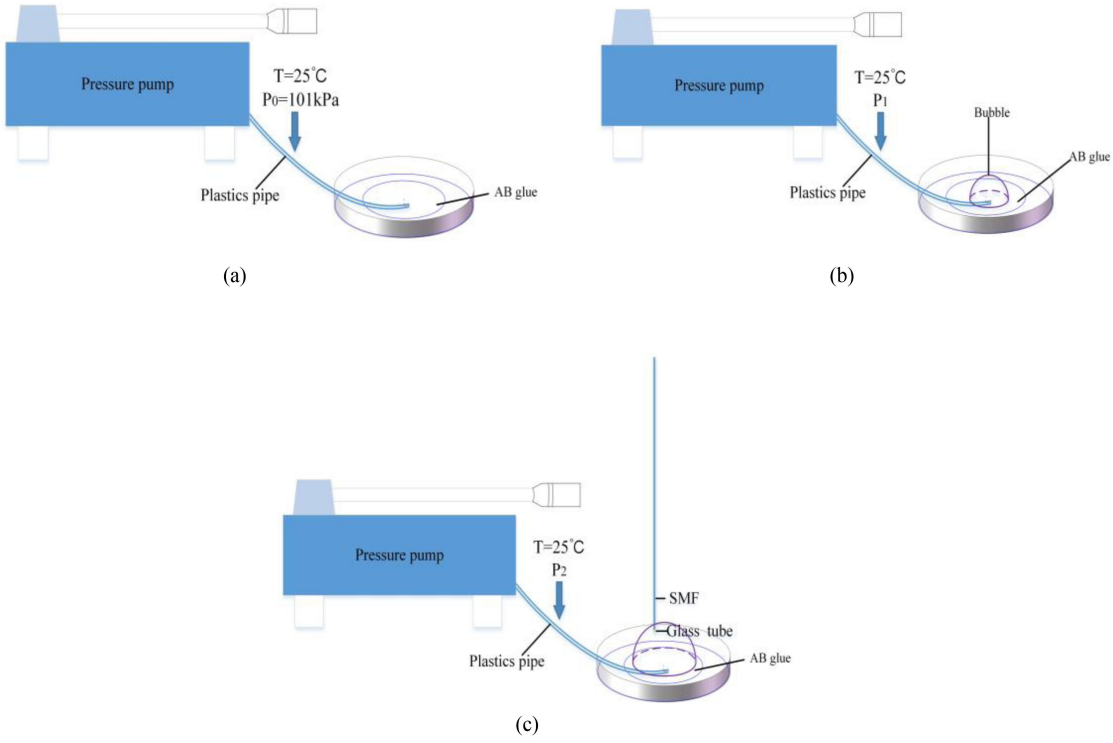

Fig. 4. **(a)** Glue mixing. (b) Increase the pressure and start blowing. (c) Film transfer.

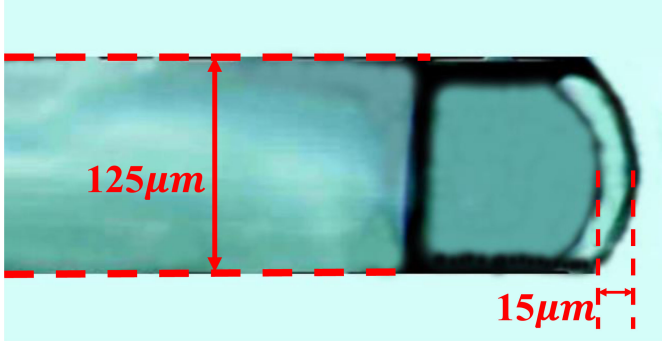

Fig. 5. The physical diagram of the samples after the transfer experiment.

light source to excite and collect the reflected light from the FP cavity, displaying a reflected image on the spectrometer. After the measurement, the thickness of the film measured by the transfer method was about 15.67 μm, which made it very sensitive to external pressure sensitivity. Fig. 6 is the physical diagram of bubble.

4. Sensor Performance Testing and Analysis

4.1 Sensor Pressure Performance Testing

After completing the above sensor preparation, the sensing characteristics of the sensor were tested. First, the gas chamber sample connected to the sensor head is placed in the pressure pump at room temperature, (thereby eliminating the influence of the temperature on the micro

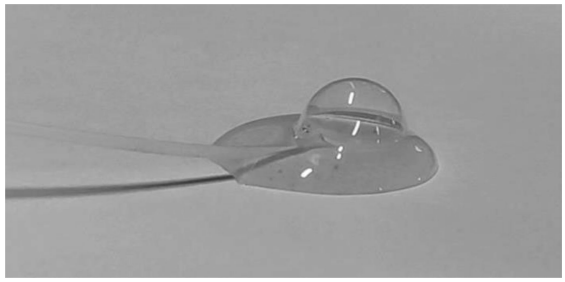

Fig. 6. The physical diagram of bubble.

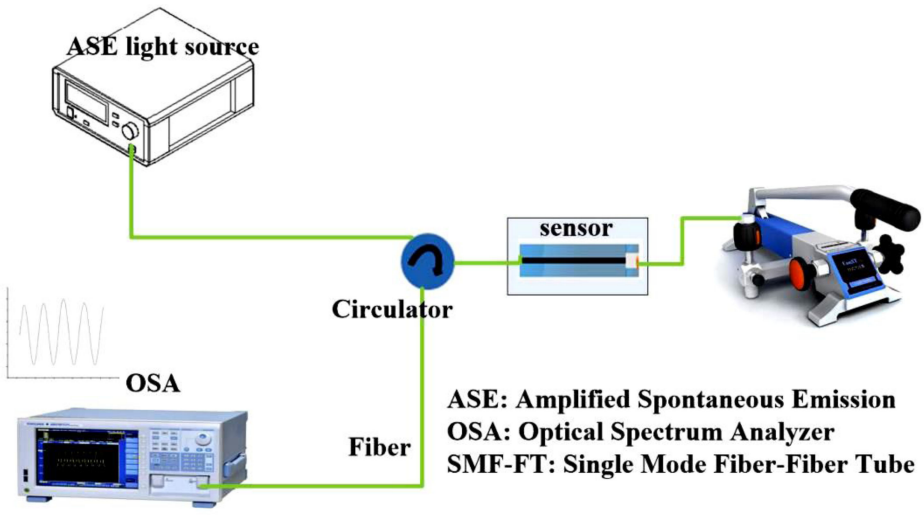

Fig. 7. The schematic diagram of the system device.

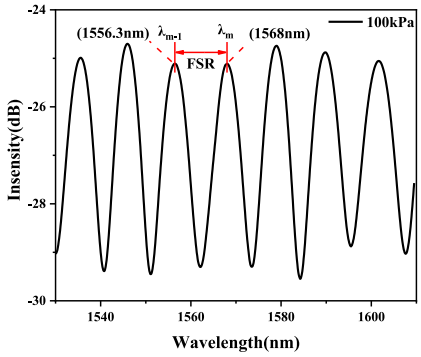

Fig. 8. Separate transmission spectrum of the fabricated sensor.

pressure test during the test) and then the peak shift of the sensor head is performed every 20 kPa in the micro pressure range of 100 kPa to 400 kPa. The experimental instruments used in this experiment include an adjustable pressure pump, a fiber fusion splicer, a broadband light source, a spectrum analyzer, and a microscope. The schematic diagram of the system device is shown in Fig. 7.

As shown in Fig. 8, we measure the FSR (free spectral range) of the interference spectrum through experiments, Interference spectra of free spectral range of 11.7 nm.

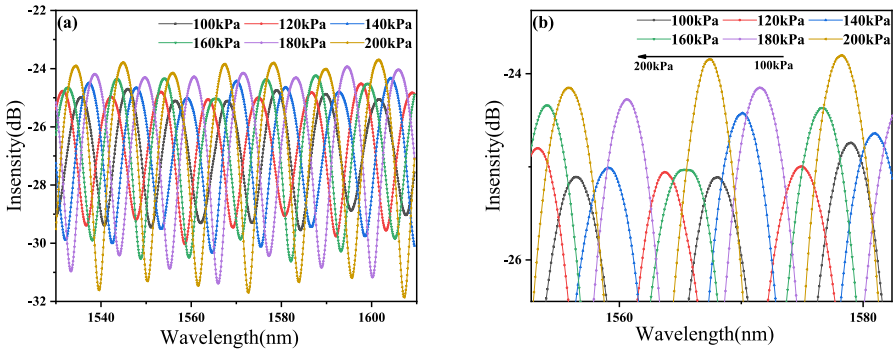

Fig. 9. (a) Local spectral characteristics of the sensor range from 100.0 kPa∼200.0 kPa. (b) Local amplification of interference of the sensor range from 100.0 kPa∼200.0 kPa.

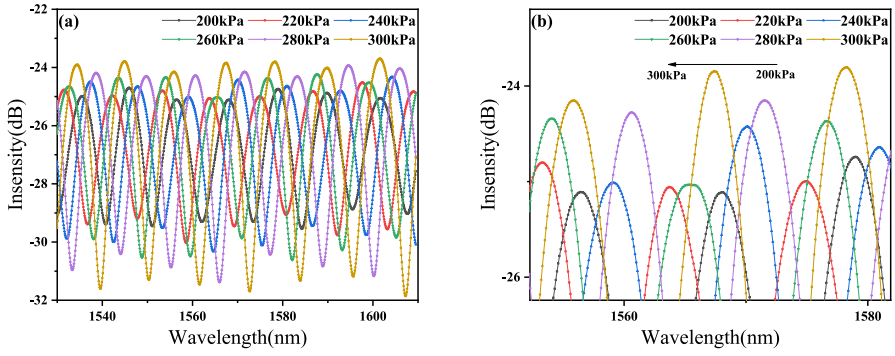

Fig. 10. (a) Local spectral characteristics of the sensor range from 200.0 kPa∼300.0 kPa. (b) Local amplification of interference of the sensor range from 200.0 kPa∼300.0 kPa.

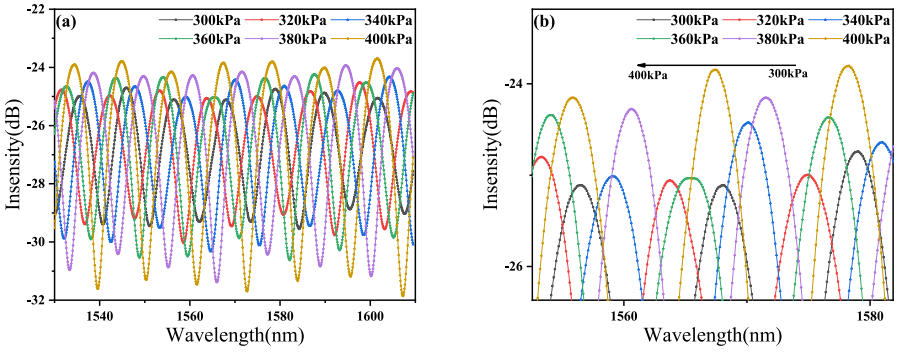

Fig. 11. (a) Local spectral characteristics of the sensor range from 300.0 kPa∼400.0 kPa. (b) Local amplification of interference of the sensor range from 300.0 kPa∼400.0 kPa.

The air chamber can be linearly pressurized by manual adjustment. The reflectance spectra of the fiber optic sensors were measured at room temperature as shown in Fig. 9(a), Fig. 9(b), Fig. 10(a), Fig. 10(b), Fig. 11(a) and Fig. 11(b). In the experiment, the reflection spectrum between 1523 nm and 1613 nm was recorded. There were multiple interference peaks in the range of 90 nm, and the interference peaks were evenly spaced, which provided more choice points for the sensor to measure the gas pressure. The use of a film on the other end of the glass tube also increases the amount of reflected light energy, resulting in an interference pattern with a more pronounced contrast. The maximum pressure was increased to 400 kPa, each time 20 kPa

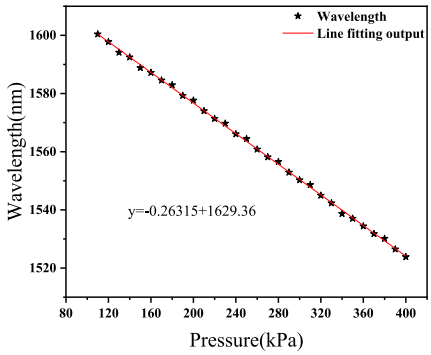

Fig. 12. Linear fitting diagram of sensor sensitivity range from 100.0 kPa∼400.0 kPa.

was added, and the spectral waveform and data were measured at each barometric measuring point for 30 s to ensure the accuracy of the measured data. As can be seen from Fig. 9(a), Fig. 9(b), Fig. 10(a), Fig. 10(b), Fig. 11(a) and Fig. 11(b), the blue-shifted of the waveform can be clearly observed when the air pressure is increased. The initial peak wavelength $\lambda_0 = 1579$ nm is selected as the observation point. It can be seen through experiment that the wavelength of the resonant peak changes significantly when the pressure changes, indicating that the sensitivity of the sensor is better. In the experiment, the OSA used is AQ6370D series of YOKOGAWA, its spectral measurement range is 600 nm∼1750 nm, and the measurement minimum precision is 0.1 nm. BBS used is the KG-ASE series of Beijing Kang Guan Century Optoelectronics Technology Co., Ltd. The spectral width is 1523 nm∼1610 nm. Based on the high elastic modulus and light transmission characteristics of AB epoxy adhesive, the AB epoxy film layer will move slightly under different pressures, which changes the cavity length of the FP cavity and the peak of the interference spectrum in the corresponding spectrometer. And the location will also change, which allows us to determine the change in pressure by detecting the offset of the interference spectrum.

Fig. 9∼Fig. 11 analyzes the sensor's reflection interference spectrum and its variation characteristics in the pressure range from 100.0 kPa to 400.0 kPa. The horizontal coordinate is the pressure, and the vertical coordinate is the wavelength. Here and as follows, we select the intermediate interference peak for more detailed analysis.

At room temperature, Fig. 12 analyzes the linear fitting characteristics of sensor sensitivity in the range of 100.0 kPa∼400.0 kPa. The horizontal coordinate is the pressure, and the vertical coordinate is the wavelength. The linearity of the curve is close to 1. The peak offset-micro pressure sensitivity can be calculated from the test data to be about 263.15 pm/kPa.

In order to explore the detection range of the sensor, we continuously increased the air pressure to 1 MPa. At this time, the film burst and the interference spectrum disappeared.

4.2 Sensor Temperature Performance Testing

Fig. 13(a) analyzes the corresponding spectral peak changes when the temperature changes. It can be seen that the interference spectrum shows a red-shifted trend when the temperature increases. Fig. 13(b) specifically analyzes the change of one of the spectral peaks when the temperature rises from 40 °C to 100 °C. It can be seen that the red-shifted trend is obvious. Fig. 14 analyzes the corresponding sensitivity characteristics of spectral peak change. The horizontal coordinate is temperature, and the vertical coordinate is wavelength. According to the curve in Fig. 14, when the temperature of the sensor head rises from 40 °C to 100 °C, the peak value is offset by 22.9 nm, and the measuring sensitivity of the sensor is about 381.7 pm/°C.

In Table I, we compare the sensitivity of pressure sensors of the similar structure in recent years. In this paper, the sensitivity of the sensor is improved obviously by using the preparation

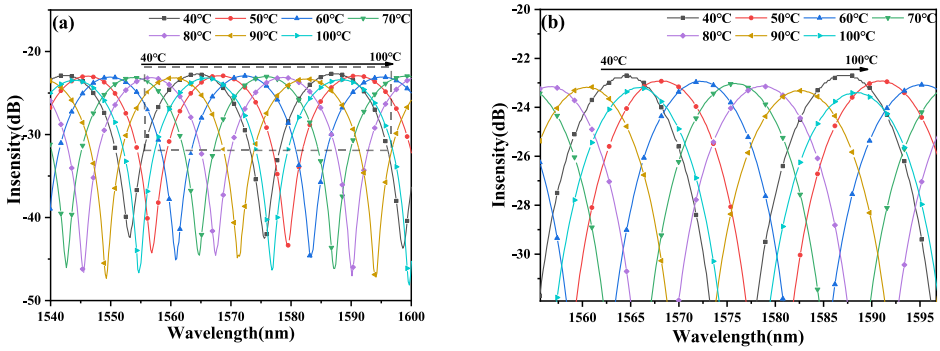

Fig. 13. (a) Global spectral characteristics of the sensor range from 40 °C∼100 °C. (b) Local spectral characteristics of the sensor range from 40 °C∼100 °C.

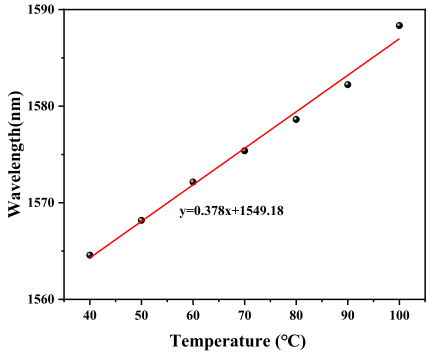

Fig. 14. Linear fitting diagram of sensor sensitivity range from 40 °C∼100 °C.

TABLE 1
The Sensitivity of Optical Fiber Fabry-Perot Pressure Sensor

Source (time, literature)	2012, Xu F, et al.	2019, Chen L et al.	2020，Shubin Z, et al.	This paper
Material	Quartz glass	PDMS	Quartz glass	AB epoxy glue
The sensitivity	315 pm/MPa	100 pm/kPa	6790 pm /MPa	263.15 pm/kPa

method. The curve is a good linear, we can think that our sensor structure has a good test performance.

5. Conclusion

The novel fiber optic pressure sensor filled with AB epoxy film based on bubble blowing method is proposed. The FP cavity is composed of the end face of the fiberglass tube and the face of the AB epoxy. The films prepared by the bubble method were thinner and less diffused than other methods, and the capillary phenomenon was effectively avoided. The total length of the sensing probe is only 30 μm–60 μm. The results show that the thickness of the thin film layer is only 15 μm, which makes it very sensitive to external pressure. And its sensing characteristics are analyzed and compared. After the pressure characteristics test, the pressure sensitivity is stable at around 263.15 pm/kPa, which is about 2.6 times of the fiber-based Fabry-Perot sensor based on PDMS filling type. Meanwhile, due to the decrease of film thickness, the sensor's resistance

to temperature interference is improved. The optical fiber Fabry-Perot pressure sensor prepared based on this method has the advantages of fast response time, ultrahigh pressure sensitivity, low cost, high stability, resistant to harsh environments, practicability and good repeatability, indicating its good application prospect in high sensitivity pressure, acoustic detection, medical field and industrial field.

Acknowledgment

The data that support the findings of this study are available from the corresponding author, upon reasonable request.

References

[1] H. Bin and G. Chao, "Research progress of optical fiber type Fabry-Perot pressure sensor," *Measuring Technol.*, vol. 32, no. 2, pp. 5–10, 2012.
[2] K. D. Reesink *et al.*, "Feasibility study of a fiber-optic system for invasive blood pressure measurements," *Catheterization Cardiovasc. Interv.*, vol. 57, no. 2, pp. 272, 2002.
[3] S. Sondergaard *et al.*, "Direct measurement of intratracheal pressure in pediatric respiratory monitoring," *Pediatr. Res.*, vol. 51, no. 3, pp. 339–345, 2002.
[4] G. Tamburrini, R. C. Di, F. Velardi, and P. Santini, "Prolonged intracranial pressure (ICP) monitoring in non-traumatic pediatric neurosurgical diseases," *Med. Sci. Monitor Int. Med. J. Exp. Clin. Res.*, vol. 10, no. 4, 2004, Art. no. MT53.
[5] S. Takeuchi *et al.*, "An optic pharyngeal manometric sensor for deglutition analysis," *Biomed. Microdevices*, vol. 9, no. 6, pp. 893, 2007.
[6] B. Romner and P. O. Grände, "Traumatic brain injury: Intracranial pressure monitoring in traumatic brain injury," *Nat. Rev. Neurol.*, vol. 9, no. 4, pp. 185, 2013.
[7] P. Roriz, O. Fraza, and O. Lobo-Ribeiro, "Antbrain injury: Intracranial pressure monitoring in traumatic brain injury," *Nat. Rev. Neurol.*, vol. 9, no. 4, pp. 893, 2013.
[8] W. Wang *et al.*, "Miniature all-silica optical fiber pressure sensor with an ultrathin uniform diaphragm," *Opt. Exp.*, vol. 18, no. 9, pp. 9006–9014, 2010.
[9] N. Wu *et al.*, "An ultra-fast fiber optic pressure sensor for blast event measurements," *Meas. Sci. Technol.*, vol. 23, no. 5, 2012, Art. no. 055102.
[10] Y. Tian *et al.*, "A miniature fiber optic refractive index sensor built in a MEMS-based microchannel," *Sensors*, vol. 11, no. 1, pp. 1078–1087, 2011.
[11] F. W. Guo *et al.*, "High-Sensitivity, high-frequency extrinsic Fabry-Perot interferometric fiber-tip sensor based on a thin silver diaphragm," *Opt. Lett.*, vol. 37, no. 9, pp. 1505–1507, 2012.
[12] F. Xu *et al.*, "Fiber-optic acoustic pressure sensor based on large-area nanolayer silver diaghragm," *Opt. Lett.*, vol. 39, no. 10, 2014, Art. no. 2838.
[13] B. Sun *et al.*, "Simultaneous measurement of pressure and temperature by employing Fabry-Perot interferometer based on pendant polymer droplet," *Opt. Exp.*, vol. 23, no. 3, 2015, Art. no. 1906.
[14] F. Yu *et al.*, "Ultrasensitive pressure detection of few -Layer MoS_2," *Adv. Materials*, vol. 29, no. 4, 2016.
[15] Z. Ran *et al.*, "Miniature fiber-optic tip high pressure sensors micromachined by 157 nm laser," *IEEE Sensors J.*, vol. 11, no. 5, pp. 1103–1106, May 2011.
[16] X. Wang *et al.*, "All-Fused-Silica miniature optical fiber tip pressure sensor," *Opt. Lett.*, vol. 31, no. 7, pp. 885–887, 2006.
[17] H. Sheng, M.-Y. Fu, T.-C. Chen, W.-F. Liu, and S.-S. Bor, "A lateral pressure sensor using a fiber Bragg grating," *IEEE Photon. Technol. Lett.*, vol. 16, no. 4, pp. 1146–1148, Apr. 2004.
[18] Y.-H. Hu *et al.*, "High sensitivity capillary structure optical fiber gas pressure sensor," *J. Optoelectron.*, vol. 6, no. 4, Art. no. 1146.
[19] K. Lingxin *et al.*, "High-sensitivity and fast-response fiber-optic micro-thermometer based on a plano-concave fabry-pérot cavity filled with PDMS," *Sensors Actuators A: Phys.*, vol. 281, pp. 236–242, 2018.
[20] M. Q. Chen, Y. Zhao, F. Xia, Y. Peng, and R. J. Tong, "High sensitivity temp. sensor based fiber air-microbubble fabry-perot interferometer with PDMS-filled hollow-core fiber," *Sensors Actuators A: Phys.*, vol. 270, pp. 60–66, Jun. 2018.
[21] Y. Zhao, M. Q. Chen, F. Xia, Y. Peng, and R. J. Tong, *Sensors Actuators A Phys.*, vol. 270, pp. 162–169, 2018.